

# EFFECTS OF ADDITIONAL UNCERTAINTIES AND HANDLING AND MITIGATION OF UNCERTAINTIES

Hieronymus HEIN

**framato**me

Hieronymus HEIN<sup>1</sup>, Julia KOBIELA<sup>1</sup>, Milan BRUMOVSKY<sup>2</sup>, Caitlin HOUTILAINEN<sup>3</sup>, Jari LYDMAN<sup>3</sup>, Bernard MARINI<sup>4</sup>, Bertrand RADIGUET<sup>5</sup>, Oleksandr STARTSEV<sup>5</sup>, Marta SERRANO GARCIA<sup>6</sup>, Rebeca HERNANDEZ PASCUAL<sup>6</sup>, Falk ROEDER<sup>7</sup>, Hans-Werner VIEHRIG<sup>7</sup>

<sup>1</sup> Framatome GmbH, Germany

<sup>2</sup> ÚJV, Czech Republic

<sup>3</sup> VTT, Finland

<sup>4</sup> CEA, France

<sup>5</sup> CNRS, France

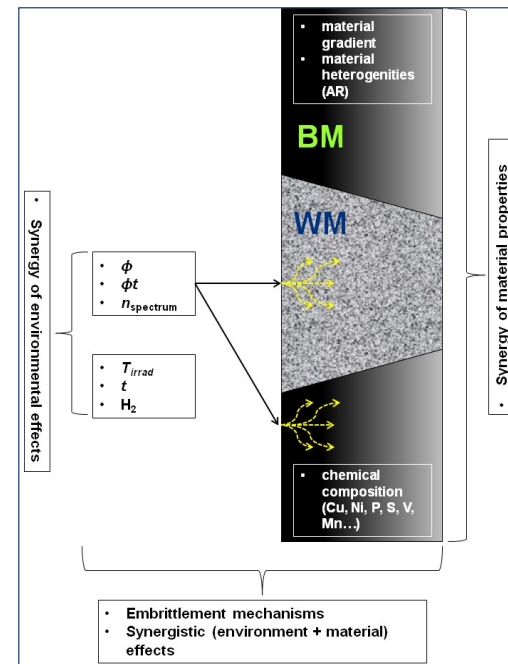
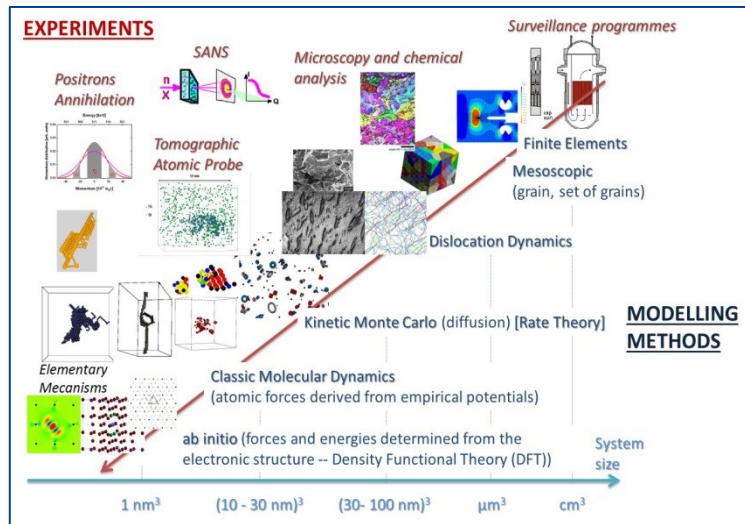
<sup>6</sup> CIEMAT, Spain

<sup>7</sup> Helmholtz-Zentrum Dresden-Rossendorf (HZDR), Germany



- ❑ Introduction
- ❑ Overview SOTERIA work package 3
- ❑ Baseline information on uncertainties in RPV irradiation embrittlement data
- ❑ Inhomogeneities in terms of mechanical properties
- ❑ Inhomogeneities in terms of composition and microstructure
- ❑ Additional uncertainties
- ❑ Conclusions

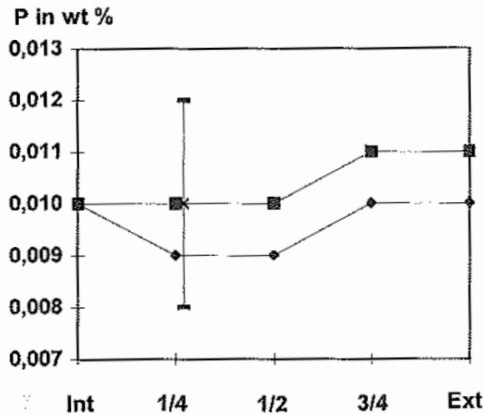
- SOTERIA WP3 “Evaluating uncertainties in fracture toughness measurement on irradiated RPV steels and mitigation approaches”
- Objective: To improve the prediction of radiation induced ageing phenomena in **RPV steels** from an end-user perspective by improvement of the applicability of the use of
  - **surveillance data**
  - modelling tools and ETCs



□ Referring to surveillance data the uncertainties in determination of RPV fracture toughness under irradiation have to be known in terms of a reliable safety assessment

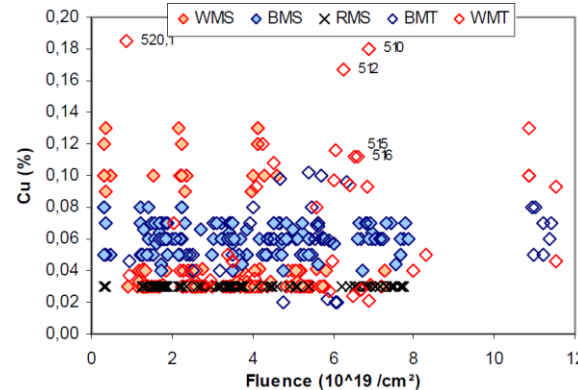
- Examples of scatter from publications (I)

*Chemical composition*



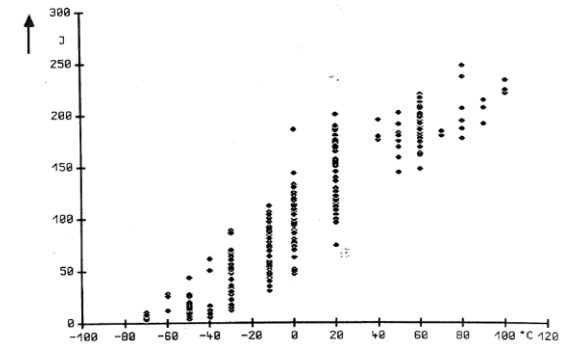
Brillaud et al, "Vessel Investigation Program of "CHOOZ A" PWR Reactor after shutdown," ASTM STP 1405, 2001

*MTR (T) vs. surveillance (S) data*



Brillaud et al, "Vessel Investigation Program of "CHOOZ A" PWR Reactor after shutdown," ASTM STP 1405, 2001

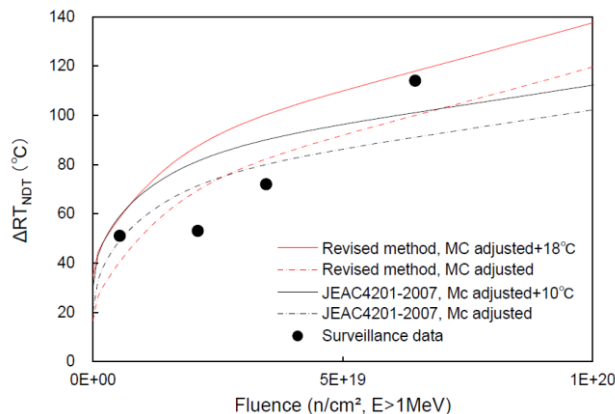
*Measured Charpy energy*



Erve, Leitz, "Irradiation behavior of RPV materials," Greifswald, 1989 - German RPV Shells, 20 MnMoNi5-5, ¼ T, T-L, 19 pre-products

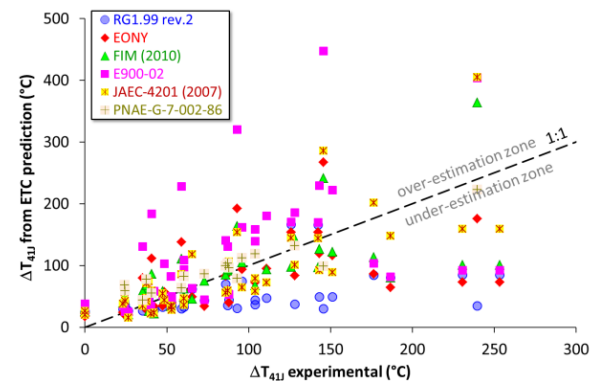
- Referring to surveillance data the uncertainties in determination of RPV fracture toughness under irradiation have to be known in terms of a reliable safety assessment
- Examples of scatter from publications (II)

*Unexpected outliers*



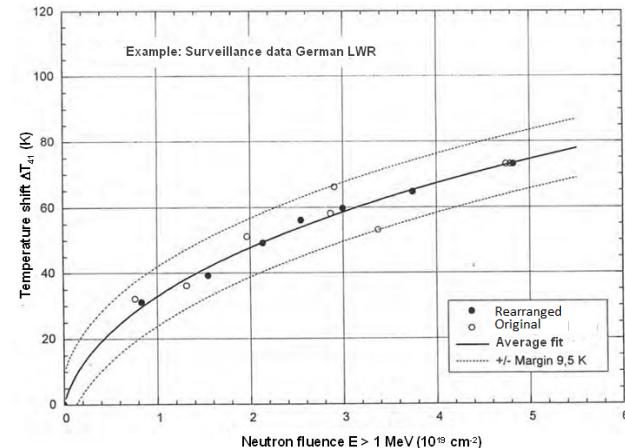
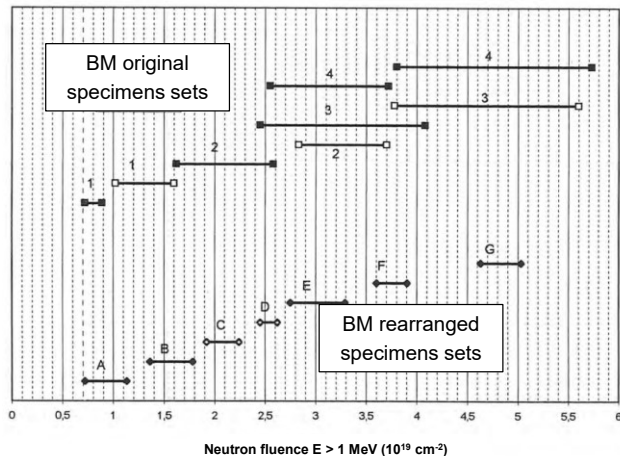
N. Soneda et al: High Fluence Surveillance Data Recalculation of RPV Embrittlement Correlation Method in Japan, PVP2013-98076, Proceedings of the ASME 2013 Pressure Vessels and Piping Conference PVP2013, July 14-18, 2013, Paris, France

*Uncertainty in predictions*

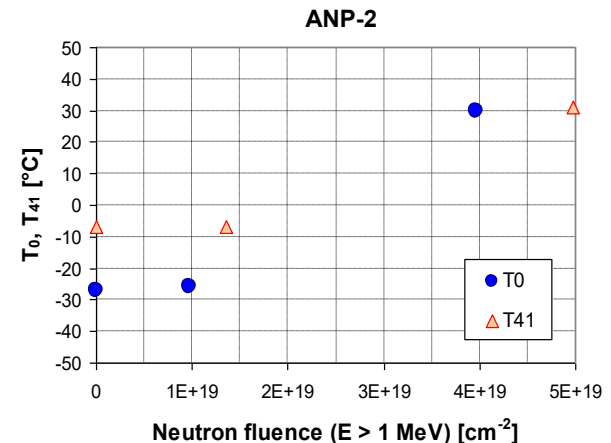


E. Altstadt et al, "FP7 Project LONGLIFE: Overview of results and implications," NED 278 (2014) 753-757

- Some additional factors affecting radiation embrittlement in surveillance specimens
  - Effect of initial heterogeneities including segregations
  - Testing conditions and number of specimens in one of the test group
  - Thermal ageing
  - Neutron flux (i.e. lead factor) and neutron energy spectrum
  - Neutron fluence distribution within one test group



- Summary of uncertainties in RPV irradiation surveillance
  - The available fracture toughness data may exhibit significant scatter
  - Additional uncertainty is then associated with differences between the data measured on surveillance specimens and the RPV itself
  - In conjunction with surveillance data, embrittlement trend curves (ETCs) are used to predict the irradiation induced change in fracture toughness and exhibit uncertainty as well
  - Macro-segregations and heterogeneous multilayer welding seams can also play an important role
  - Unexpected high irradiation embrittlement and outliers observed occasionally in both surveillance and materials test reactor(MTR) data



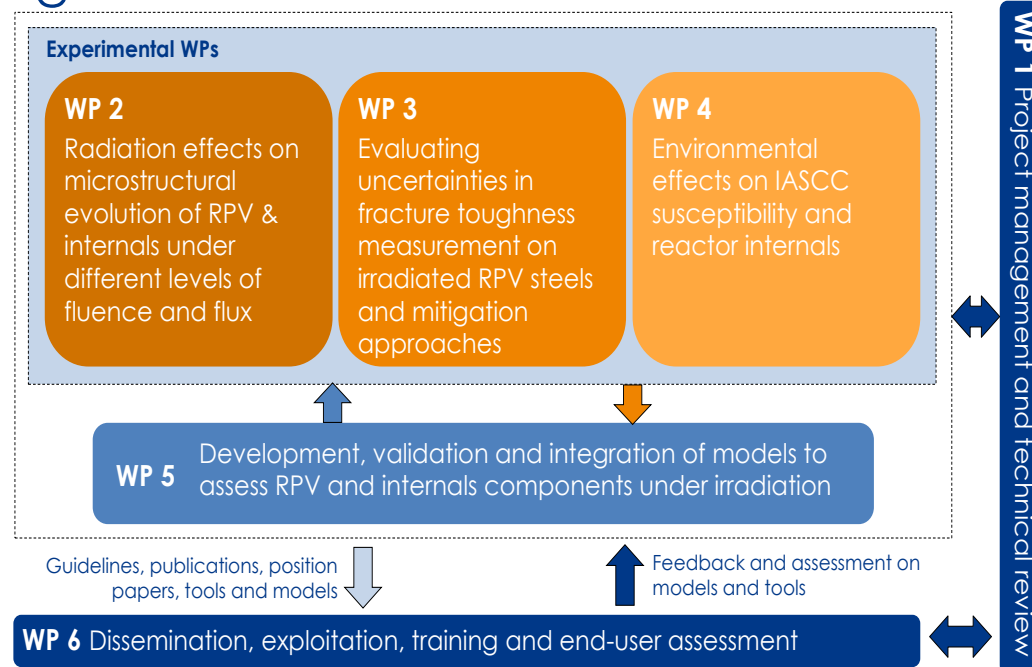
H. Hein, E. Keim, J. May, H. Schnabel, Some recent research results and their implications for RPV irradiation surveillance under long term operation, IAEA Technical Meeting on Degradation of primary components of Pressurised Water Cooled Nuclear Power Plants: current issues and future challenges, 5-8 November 2013, Vienna, Austria

# Overview SOTERIA WP3



## □ SOTERIA (Safe long term operation of light water reactors)

- Aims to address these uncertainties through work performed in work package WP3



C. Robertson, SOTERIA project, presented at Nuclear Days 2018 – NUGENIA Annual Forum, Prague, Czech Republic, April 10-12, 2018, <http://nugenia.org/look-back-at-nuclear-days-and-nugenia-forum/>.





- SOTERIA WP3 (Evaluating uncertainties in fracture toughness measurement on irradiated RPV steels and mitigation approaches)
  - Task 3.1: Baseline information on uncertainties in RPV irradiation embrittlement data
  - Task 3.2: Microstructural characterisation and impact on mechanical material properties at initial state
  - Task 3.3: Effects of initial materials inhomogeneities on microstructure and mechanical properties at irradiated state of LTO
  - Task 3.4: Effects of additional uncertainties in RPV surveillance data
  - Task 3.5: Applications and guidance for handling and mitigation of uncertainties

## □ RPV materials investigated

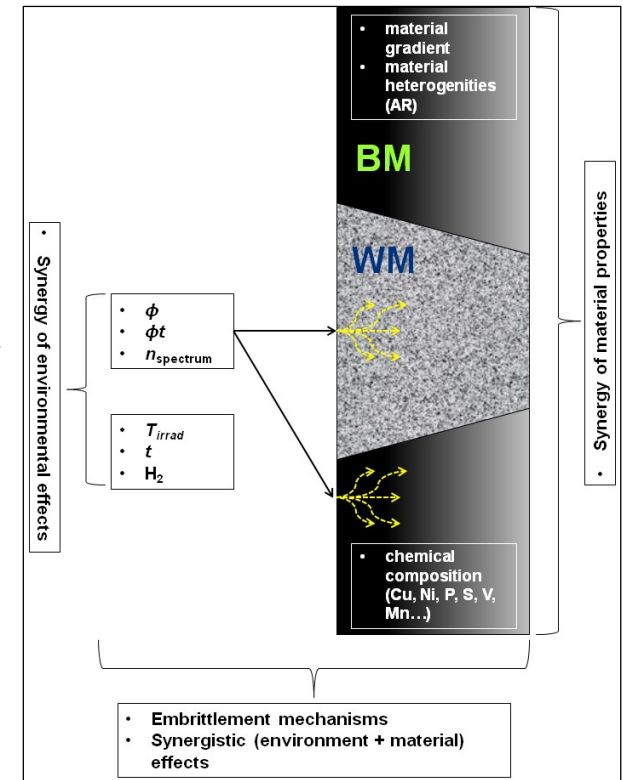
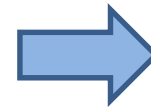
- A significant number of representative unirradiated and irradiated RPV steels used in European Light Water Reactors (LWR) were studied

Material ID	Material	Remark
ANP-2	S3NiMo1/OP41TT	WM, outlier observed at 4.97 n/cm <sup>2</sup> (E > 1 MeV)
ANP-3	22NiMoCr3-7	BM, Kloeckner
ANP-4	22NiMoCr3-7	BM, reference material JSW
ANP-5	NiCrMo1/LW320, LW330	WM, test weld seam, high Cu
ANP-6	S3NiMo/OP41TT	WM, Uddcomb, high Ni
ANP-10	22NiMoCr3-7	BM
ANP-15	22NiMoCr3-7	BM, Kloeckner, 30 years thermally aged
CIE-01	SA-508 Cl.3	BM, MnMoNi steel
EDF-4	16MnD5	BM, CrMoV steel
FZD-1b	A533B Class 1	JPC (Japanese A533B Class 1 material), low P
FZD-2	10Kh2MFT	WM (WWER-440/V-230) Greifswald unit 4, Ishora, K <sub>Jc</sub> scatter T-S
FZD-3	15Kh2MFA	BM (WWER-440/V-230) Greifswald unit 4, Ishora, K <sub>Jc</sub> scatter L-S
FZD-4	15Kh2MFAA	BM (WWER-440/V-213) Greifswald unit 8, Skoda, K <sub>Jc</sub> scatter
JRQ	A 533-B	BM (IAEA reference steel)
JRQ UJV-2	Sv 12Kh2N2MAA / 15Kh2NMFA	WWER steel
UJV-2	15Kh2NMFA	WM (WWER-1000)
VFAB 1	S3NiMo/OP41TT	WM, Uddcomb, high Ni
VTT-1	10KhMFT	WM (WWER-440), high Cu
VTT-MW1	10KhMFT	WM (mock-up weld, WWER-440), high P content

# Baseline information on uncertainties in RPV irradiation embrittlement data



- Mechanical properties of the irradiated RPV materials
  - are also dependent on initial micro- and macrostructure and on the RPV manufacturing process
  - are fraught with uncertainties linked to incomplete information about the RPV's initial micro- and macrostructure and manufacturing conditions
  - Synergistic effects between environmental and material factors on RPV irradiation embrittlement
- Survey conducted in SOTERIA
  - Initial material heterogeneities and chemical composition identified as most significant uncertainties in RPV embrittlement data
  - Test matrix for the experimental work, in particular to study the effects of materials heterogeneities on the mechanical properties of RPV steels at both initial irradiated state

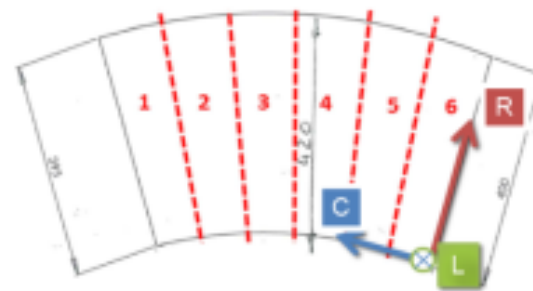
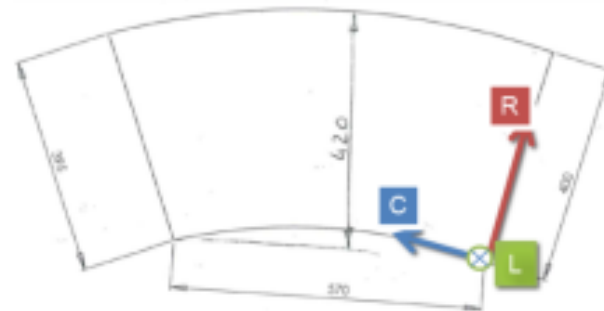
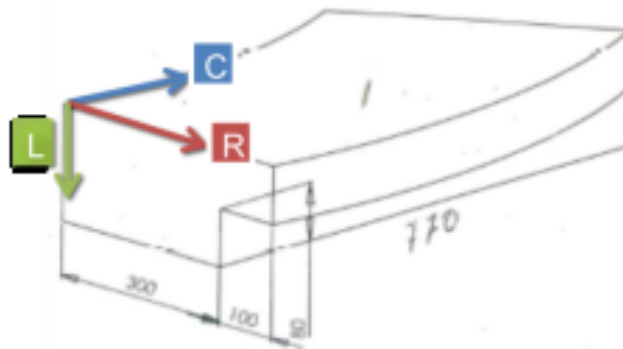


# Inhomogeneities in terms of mechanical properties



## □ Tensile tests

- Tensile properties may depend on the circumferential location as observed for tensile strength in **CIE-1** forging.



# Inhomogeneities in terms of mechanical properties



## □ Tensile tests

- Tensile properties may depend on the circumferential location as observed for tensile strength in CIE-1 forging.
- Tensile properties (yield strength, ultimate tensile strength, and fracture stress) may depend on the RPV wall depth as observed for UJV-1.
- However, tensile properties practically do not depend on the depth in the wall for UJV-2 – could be caused by different quenching rates on both cylindrical ring surfaces.
- No effect of specimen location was observed for FZD-4 material.

Material	N° specimens	Ultimate Tensile Strength (MPa)		
		UTS (MPa) [ASTM E8 error= 1.30%]		
		Average	SD	Error
JRQ RT	13	644	23	4%
UJV-2 RT	11	568	8	1%
CIE-1 T=-100 °C	7	760	12	2%
CIE-1 T=-50 °C	8	693	8	1%
CIE-1 T=0 °C	8	649	7	1%
CIE-1 RT	12	626	5	1%
CIE-1 290	12	632	5	1%
FZD-4 T=100 °C	3	606	6	1%
FZD-4 RT	8	648	10	2%
FZD-4 T=-15 °C	3	678	2	0%
FZD-4 T=-40 °C	3	703	7	1%
FZD-4 T=-65 °C	3	732	5	1%
FZD-4 T=-90 °C	3	754	22	3%
FZD-4 T=-100 °C	3	774	2	0%
FZD-4 T=-115 °C	3	809	1	0%
FZD-4 T=-140 °C	3	854	31	4%

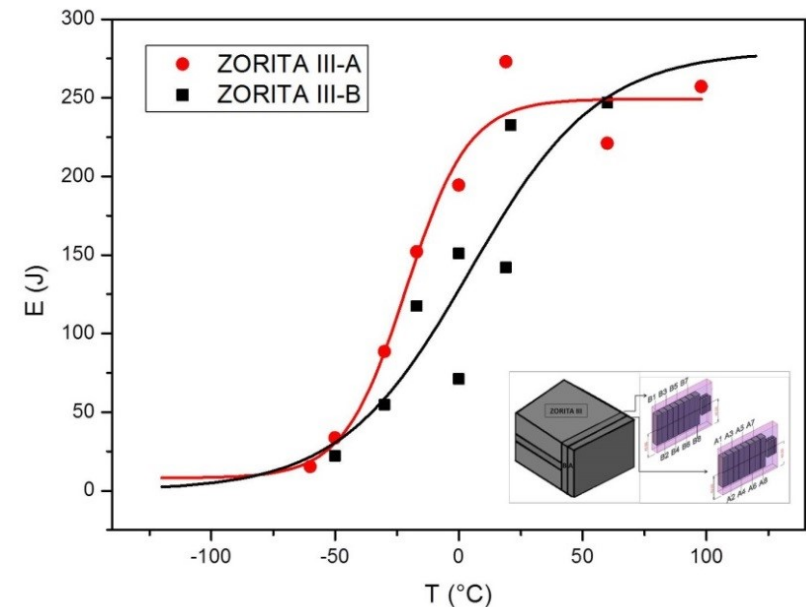
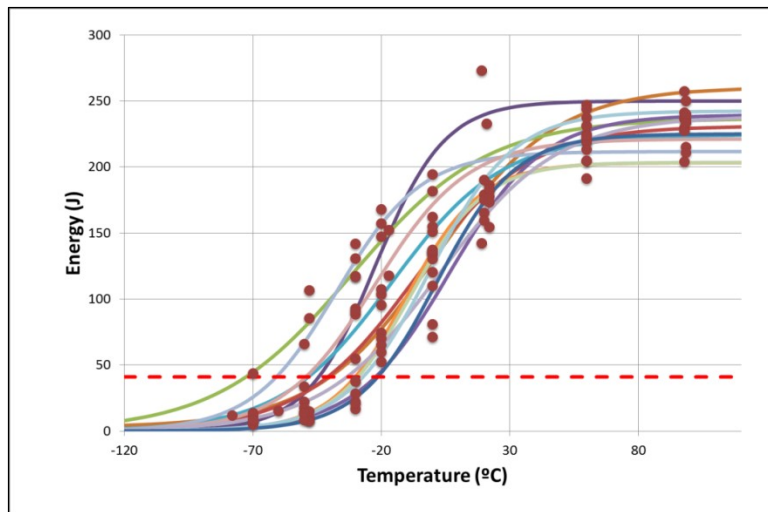


# Inhomogeneities in terms of mechanical properties



## □ Charpy tests

- The Charpy impact tests on CIE-1 material from different locations show a dependence of the absorbed energy and a shift in the transition curve with the location of the specimens



# Inhomogeneities in terms of mechanical properties



## □ Charpy tests

- Material CIE-1
- Average  $T_{41} = -41$  °C with a standard deviation of 14 °C.
- Average USE = 230 J with a standard deviation of 17 J.
- $T_{41}$  depends on specimens' location on R-axis that can be explained by different cooling rate through thickness of the ingot during forging fabrication

Group	Coord C (mm)	Coord R (mm)	Coord L (mm)	$T_{41}$ (°C)	USE (J)
T4-III-A	190	388	40	-45	250
T4-III-B	190	375	40	-40	261
T5-II-A	95	12	130	-41	231.1
T5-II-B	95	27	130	-73	236.8
T5-II-C	95	134	130	-46	234
T5-II-D	95	149	130	-22	239
T5-II-E	95	255	130	-49	224
T5-II-F	95	270	130	-30	203
T6-II-A	0	12	130	-61	211.7
T6-II-B	0	27	130	-49.5	221.2
T6-II-C	0	134	130	-29	203
T6-II-D	0	149	130	-34	239
T6-II-E	0	255	130	-34	242
T6-II-F	0	270	130	-22	225

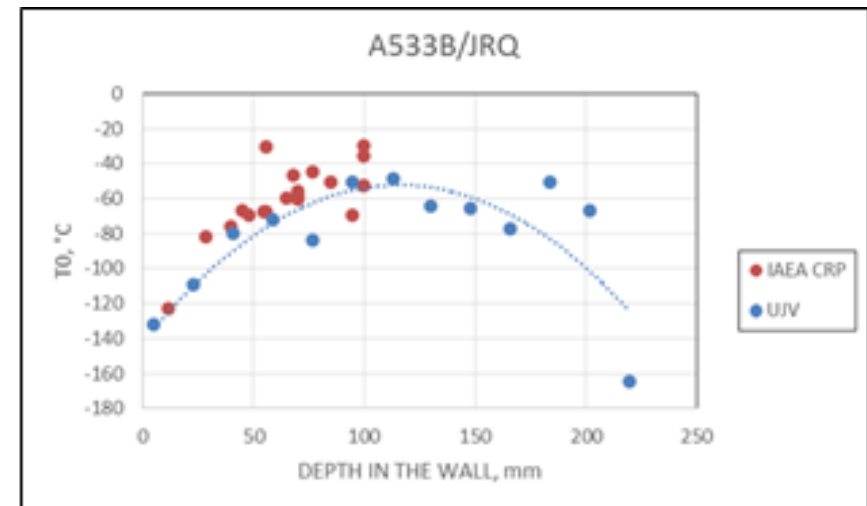
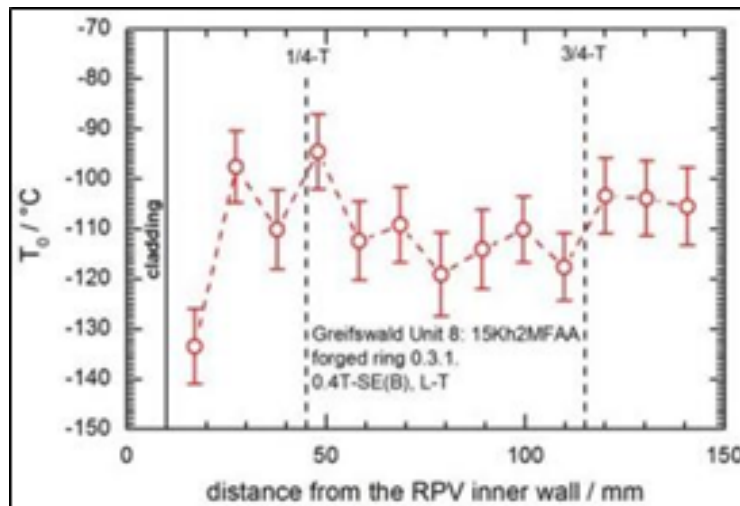


# Inhomogeneities in terms of mechanical properties



## □ Fracture toughness tests (ASTM E1921)

- Usually the standard deviation is between 7 and 9 °C that was measured for FZD-4 and UJV-1 (JRQ) materials.
- The additional standard deviation of  $T_0$  through the RPV wall between  $\frac{1}{4}$  and  $\frac{3}{4}$  thickness was determined to 8 °C (10 °C for full thickness) for FZD-4 (left) and 12 °C (33 °C for full thickness) for UJV-1 (right).



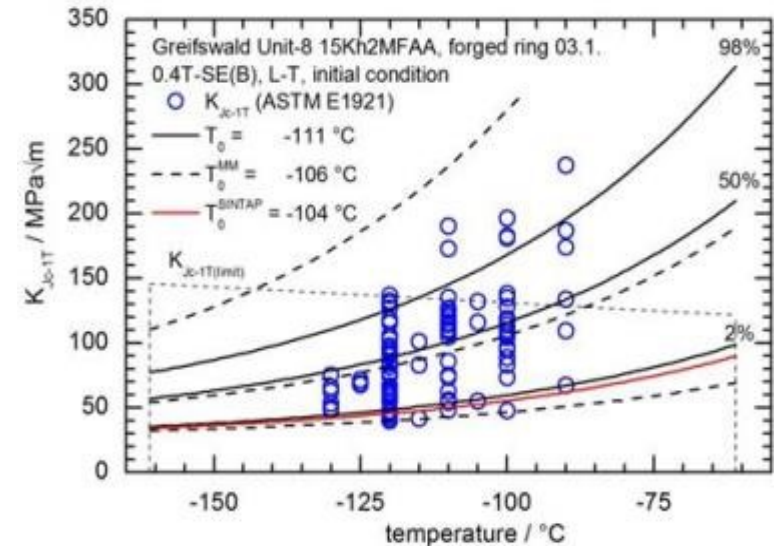


# Inhomogeneities in terms of mechanical properties



## Fracture toughness tests (ASTM E1921)

- FZD-4: 98 0.4T SE(B) specimens sampled between 1/4 to 3/4 thickness were summarized to one dataset ( $T_0 = -111 \text{ }^\circ\text{C}$ )
- Dataset was evaluated according to Master Curve based SINTAP and multimodal approaches
- $MLNH > 2$  indicates the material as non-homogeneous



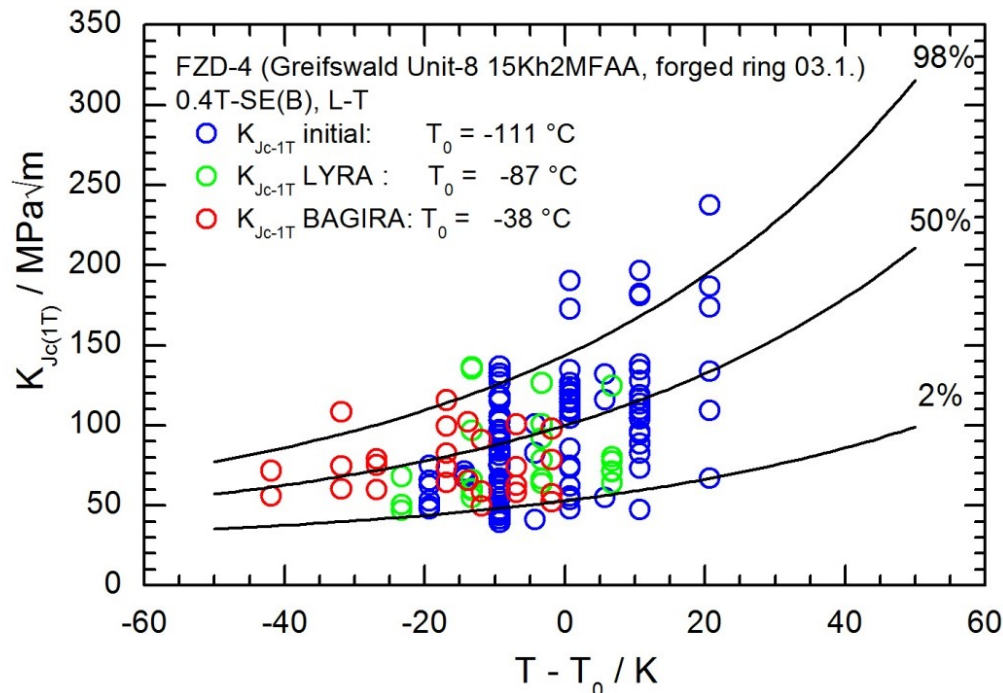
specimen type	condition	N	SINTAP		$T_0^{MM}$ °C	$\sigma$ °C	multimodal		MNLH
			$T_0^{SINTAP}$ °C	$K_{Jc-1T}$ MPa√m < 2 %			$K_{Jc-1T}$ MPa√m < 2 %   > 98 %		
0.4T-SE(B) L-T	initial	98	-104	6	-106	19	4   0	10.6	



# Inhomogeneities in terms of mechanical properties



- Fracture toughness at testing according to ASTM E1921 (Master Curve approach)
  - FZD-4 results (0.4T SE(B) specimens) indicate a lower material inhomogeneities for the irradiated material conditions



LYRA:  $\Phi = 2.07 \cdot 10^{19} \text{ n/cm}^2$ ,  $E > 1\text{MeV}$ ,  $T_{irr} = 270^\circ\text{C}$

BAGIRA:  $\Phi = 11.7 \text{ to } 28.2 \cdot 10^{19} \text{ n/cm}^2$ ,  $E > 1\text{MeV}$ ,  $T_{irr} = 290^\circ\text{C}$

$K_{Jc-1T}$  values outside 2% and 98%:

- initial condition: 19 out of 98 (19%)
- LYRA irradiation: 2 out of 22 (9%)
- BAGIRA irradiation: 2 out of 26 (8%)



# Inhomogeneities in terms of mechanical properties



## □ Fracture toughness tests (ASTM E1921)

### • Conclusions

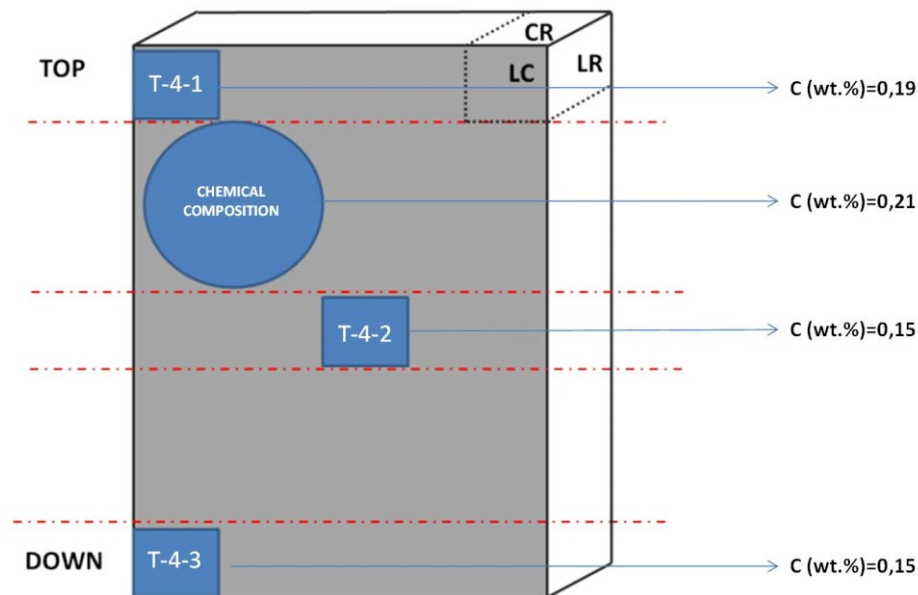
- Typical standard deviation for  $T_0$  is less than 10 °C, whereas the wall location itself can result in an additional standard deviation for  $T_0$  of about 10 °C.
- Basically, the requirement of the RPV surveillance standards to take the surveillance specimens in the  $\frac{1}{4}$  to  $\frac{3}{4}$  thickness range was confirmed by the test results.
- The IAEA Guideline TRS No. 429 offers further guidance in evaluation of uncertainties of  $T_0$  determination including margin.
- Inhomogeneity checks for  $T_0$  show a reduced number of outliers but an increase of  $T_0$  by using the SINTAP and multi modal approaches (newer editions of ASTM E1921 involve inhomogeneity checks!).



# Inhomogeneities in terms of mechanical properties



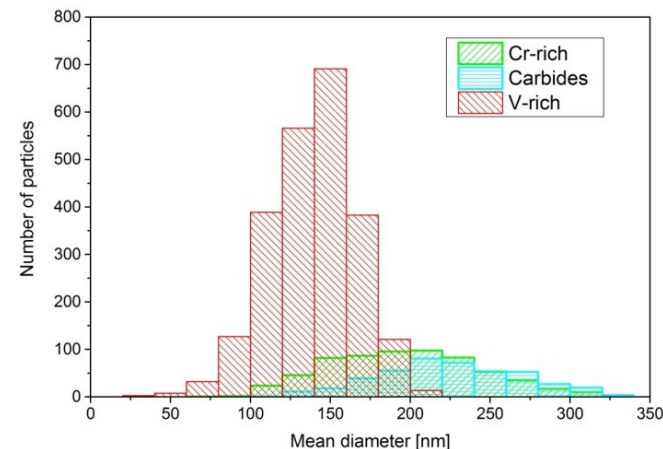
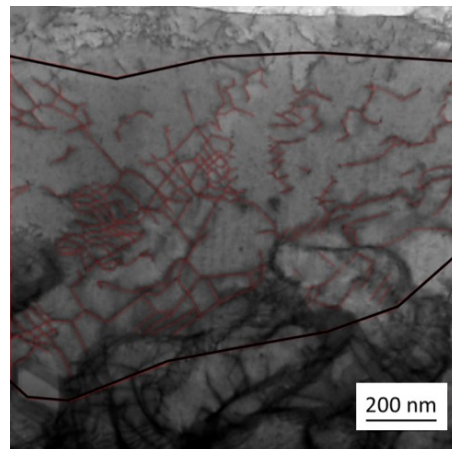
- Inhomogeneities in terms of composition and microstructure
  - CIE-1: Chemical analysis of the carbon content in different areas of the slice revealed different carbon contents
  - May be caused by solidification process, first occurring in the lower and outer parts of the ingots (lower carbon)



# Inhomogeneities in terms of composition and microstructure



- Inhomogeneities in terms of composition and microstructure
  - FZD-4: TEM microstructure – dislocation lines are tracked by thin red lines and the region by thick black lines (left), distribution of mean particle diameter for Cr-rich precipitates, carbides and V-rich precipitates (right)
  - Some precipitates (e.g. P) preferentially located at grain boundaries may be related to large fractions of intergranular fracture observed in mechanical tests



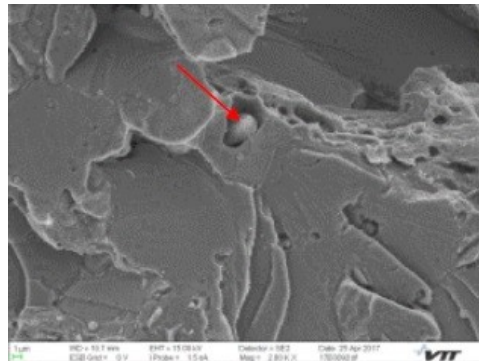
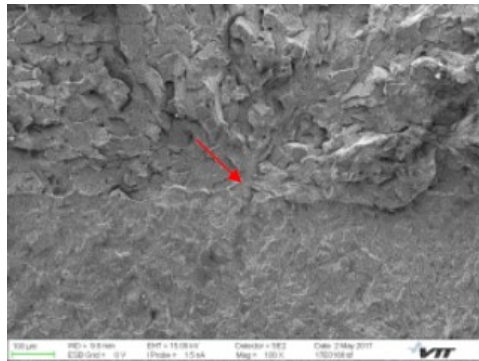
# Inhomogeneities in terms of composition and microstructure



## □ Material heterogeneities

- Role of non-metallic inclusions
- Role of specimen thickness if the specimen size is smaller than the distance between the heterogeneities (if any)

For **ANP-3/-4** the primary initiation site is not characterized by a specific microstructural feature (precipitate or inclusion), whereas for **VTT-1** the initiation sites of two specimens revealed a brittle Si and Mn rich particle.



# Inhomogeneities in terms of composition and microstructure



## □ Material heterogeneities

- SEM fractography

- Fracture initiation sites

- particles in some cases, but not necessarily carbides as assumed in some fracture models
    - multi element particles consisting of Mn, Mo, S, Cr, Al, C and O

Material	Specimen	Initiation site	Particle type
ANP-3	BA28	Primary Initiation site Not visible, as it locates under a ledge	No visible particle
ANP-3	BA32	Primary initiation site particle	Cr-, Mn-, Mo- (+ S), Co- and O-rich particle Cr, Mn, Co = half A Mo (+ S), O = half B
ANP-3	BA35	Primary initiation site particle	Probably a Mn-, Cr-, Mo- (+ S), Al-, O-rich particle half A only no particle on half B
ANP-4	2BTL3	Primary initiation site	No clear particle
ANP-4	2BTL9	Primary initiation site particle	Probably a Mn-, Mo- (+ S), S-, Cr-, C- and O-rich particle Mo (+ S), Cr, Mn, O = half A Mo, S, Cr, Mn, O = half B
ANP-4	2BTL14	Primary initiation site	No particle visible
VTT-1	L22_17I209	Initiation site	No particle visible
VTT-1	L22_18I204	Initiation site Particle	Al-, Si-, S-, Ti-, Mn- and O-rich particle
VTT-1	L24_17I204	Initiation site Particle	Al-, Si-, Ti-, Mn- and O-rich particle
VTT-MW1	132M	Initiation site Particle	Al-, Si-, Ti-, V-, Mn- and O-rich particle
VTT-MW1	172	Initiation site Particle	Al-, Si-, Ti-, Mn- and O-rich particle
VTT-MW1	311	Initiation site Particle	Si- and O-rich particle

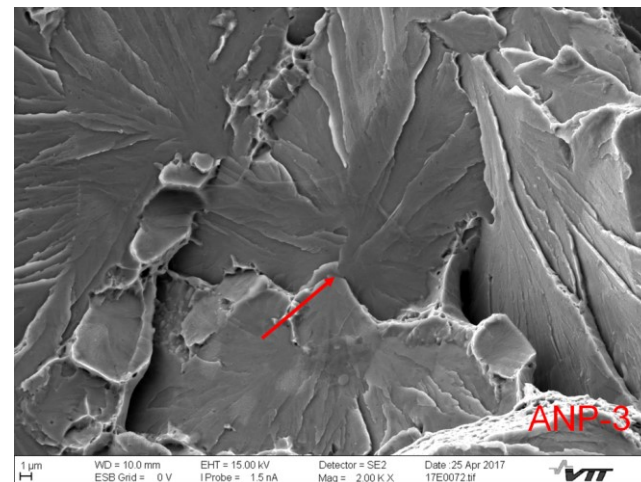
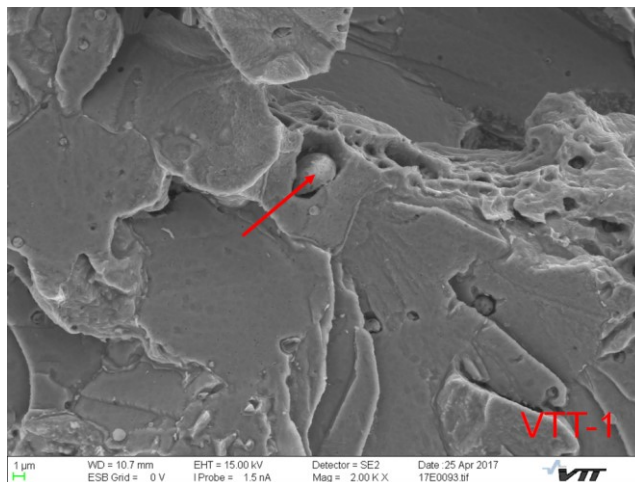


# Inhomogeneities in terms of composition and microstructure



## □ Fractographic analysis

- SEM fractography with primary initiation sites of weld metal VTT-1 (left) and base material ANP-3 (right)
  - ANP-3: There was one specimen for each base material where the fracture was most likely, or could have been, initiated by a particle, but not by a specific microstructural feature, such as precipitate or inclusion
  - VTT-1: Initiation sites of two specimens revealed a brittle Si and Mn rich particle, whereas a round ductile, Al, Si, Ti and Mn rich particle was found at the initiation site of the third sample, but no specific microstructural feature, such as precipitate or inclusion, at which brittle fracture initiated





## □ Chemical analyses

- There are two main uncertainties to be considered in chemical analyses: the measurement method itself and the material variability.
- Chemical analyses were performed on unirradiated and irradiated low Cu/Ni/P materials ANP-2 and ANP-4 (5 samples each) and high Ni weld VFAB-1 (3 samples each), using optical emission spectroscopy (OES) and inductively coupled plasma mass spectroscopy (ICP-MS) methods.

## □ Chemical analyses

- Unirradiated ANP-2 and ANP-4 materials
- Non-negligible uncertainty compared to heat analysis at manufacture was found for some chemical elements that may effect ETC predictions, particularly when Cu, Ni and P content are input parameters

<b>ANP-2</b>	<b>C [%]</b>	<b>Mn [%]</b>	<b>P [%]</b>	<b>S [%]</b>	<b>Ni [%]</b>	<b>Cu [%]</b>
average measured by OES	0,0607	1,052	0,0167	0,0054	1,020	0,034
σ [%]	4,06	2,46	6,49	3,58	1,20	3,55
heat at manufacture	0,05	1,08	0,019	0,009	1,01	0,03
relative deviation [%]	21,4	-2,6	-12,2	-40,2	1,0	14,7

<b>ANP-4</b>	<b>C [%]</b>	<b>Mn [%]</b>	<b>P [%]</b>	<b>S [%]</b>	<b>Ni [%]</b>	<b>Cu [%]</b>
average measured by OES	0,182	0,925	0,0045	0,0045	0,886	0,063
σ [%]	1,47	0,51	4,44	21,02	1,32	2,45
heat at manufacture	0,21	0,85	0,006	0,006	0,84	0,05
relative deviation [%]	-13,2	8,8	-25,0	-25,0	5,5	27,0



## □ Chemical analyses

- Unirradiated ANP-2 and ANP-4 materials
  - Uncertainty of the OES analyses (5 single measurements each)
    - NORDTEST procedure through repeated measurements on 10 certified reference materials resulting in an extended relative uncertainty  $u$  where differences between the measured value and the certified value of the element content, together with variations in repetitive measurements and the uncertainty of the reference material are being considered.
    - The extended relative uncertainty  $u$ , a multiplication of the standard uncertainty and the extension factor  $k = 2$ : [REDACTED]

Extended relative uncertainty	P [%]	Cu [%]	C [%]	Mo [%]	Cr [%]	Ni [%]	Mn [%]
ANP-2	59	42	14	10	8	7	5
ANP-4	59	42	14	10	9	7	5

- Reason for the higher  $u$  values might be the low original element concentrations (around  $\sim 0.1$  mass. %), which is close to the detection limit of OES analyses. Nevertheless, for Mn, Ni and Cr the relative uncertainties are in the range between 5 and 8 % (see previous slide).

## □ Chemical analyses

- Unirradiated and irradiated VFAB-1 (high Ni): OES, ICP

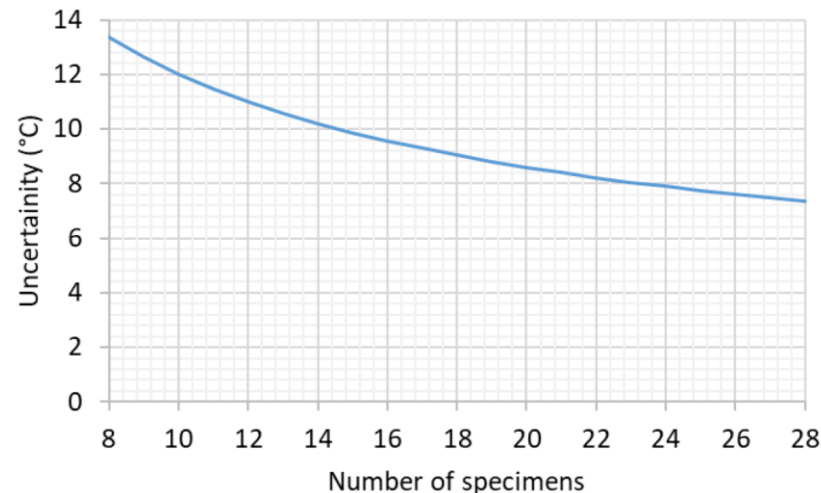
VFAB-1	Fluence (E> 1MeV) cm <sup>-2</sup>	Sample ID	C	Si	Mn	P	S	Cr	Mo	Ni	Al	Co	Cu	V	Sn	Fe
AREVA 2015/OES	~3E18	R2	0,063	0,21	1,66	0,016	0,005	0,14	0,38	1,08	0,03	0,01	0,06	0,01	-	96,3
AREVA 2015/OES	~3E18	A7	0,09	0,21	1,52	0,012	0,006	0,14	0,41	1,08	0,02	0,01	0,08	0,01	-	96,3
AREVA 2015/OES	~3E18	G4	0,072	0,21	1,55	0,015	0,006	0,13	0,39	1,27	0,02	0,01	0,06	0,01	-	96,2
AREVA 2016/ICP	~3E18	R2	0,067	0,197	1,55	0,013	0,006	0,127	0,419	1,69	0,019	0,008	0,057	0,007	-	96,3
AREVA 2016/ICP	~3E18	A7	0,103	0,193	1,49	0,011	0,007	0,131	0,436	1,43	0,017	0,012	0,075	0,004	-	96,3
AREVA 2016/ICP	~3E18	G4	0,073	0,208	1,52	0,013	0,006	0,129	0,425	1,64	0,02	0,009	0,055	0,005	-	96,8
AREVA 2016/OES	0	R3	0,08	0,22	1,63	0,014	0,006	0,13	0,38	1,61	0,02	0,01	0,07	0,01	-	95,8
AREVA 2016/OES	0	A6	0,118	0,22	1,52	0,01	0,007	0,13	0,41	1,33	0,02	0,02	0,09	0,006	-	96,1
AREVA 2016/OES	0	G3	0,058	0,23	1,83	0,019	0,008	0,14	0,25	1,46	0,04	0,03	0,07	0,01	-	95,7

▾ OES



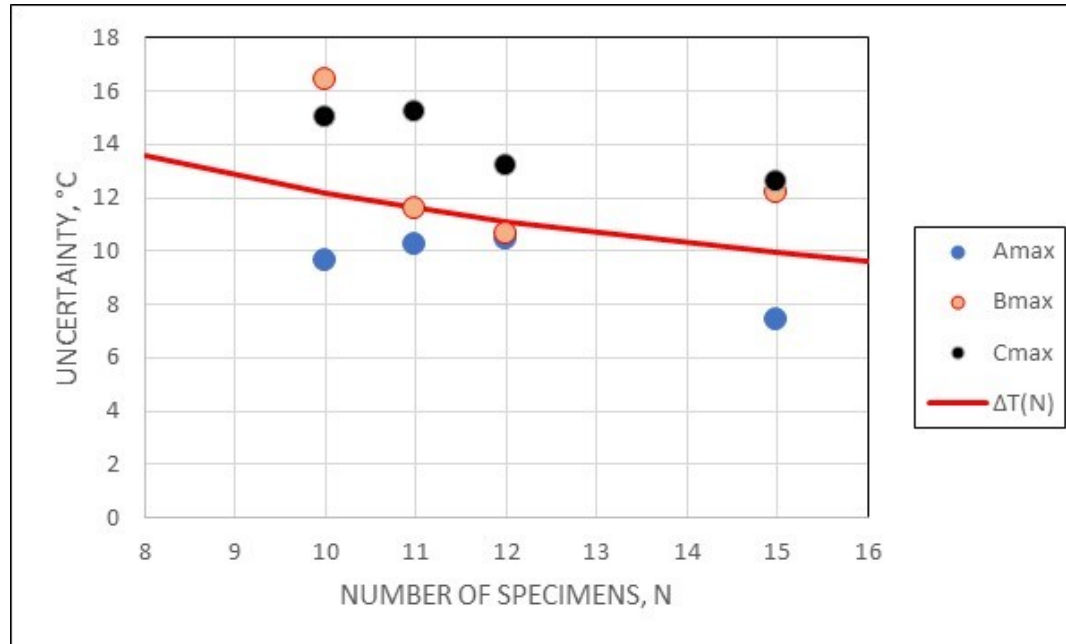
Non-negligible deviations for Cu, Ni and P may affect ETC predictions

- Impact of the test matrix on the uncertainty of the Charpy transition temperature
  - Number of available specimens, the choice of test temperatures and the number of specimens at each test temperature
  - Monte Carlo method for analysis of an impact energy database (141 tests) of a representative RPV steel similar to EDF-4 giving  $\sim 10$  °C uncertainty for transition temperature ( $T_{41}$ )



$$\Delta T(n) \approx \frac{38.5}{\sqrt{n}}$$

- Impact of the test matrix on the uncertainty of the Charpy transition temperature
  - Dependence of the uncertainty in the computation of transition temperatures  $T_{41}$  on the number of specimens in the group and comparison with the prediction for  $\Delta T(N)$ 
    - A – weld Sv-10KhMFT, B – steel 15Kh2NMFAA, C – weld Sv-12Kh2N2MAA



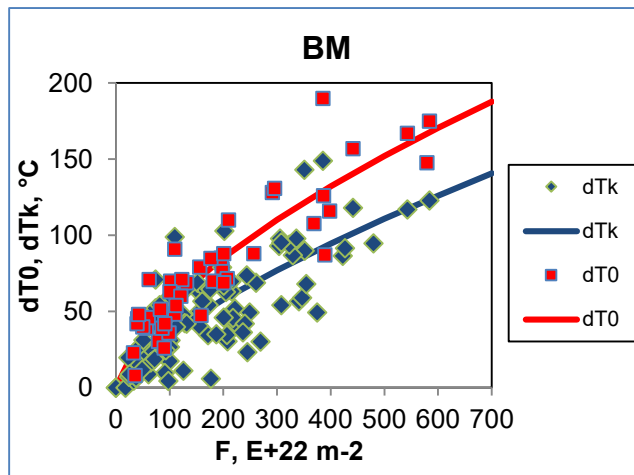
$$\Delta T(n) \approx \frac{38.5}{\sqrt{n}}$$

## □ Scatter between fracture toughness and Charpy impact shifts

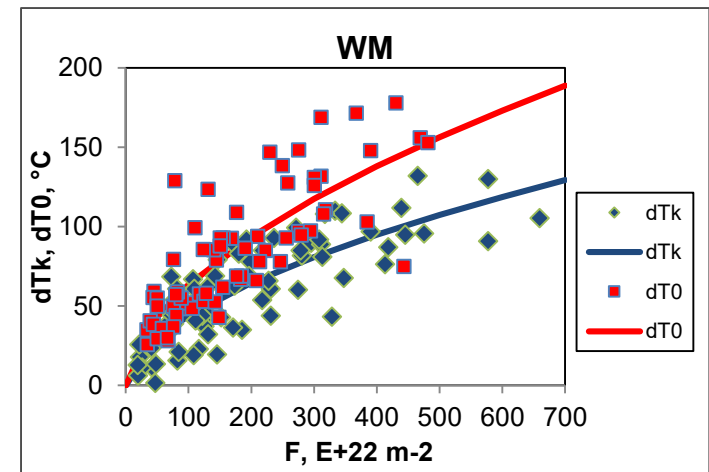
### • Sources

#### ▪ Scatter due to

- heterogeneities within the specimen group for one type of testing
- heterogeneities between two groups of specimens
- differences in irradiation of these two groups of specimens
- uncertainties of test parameters



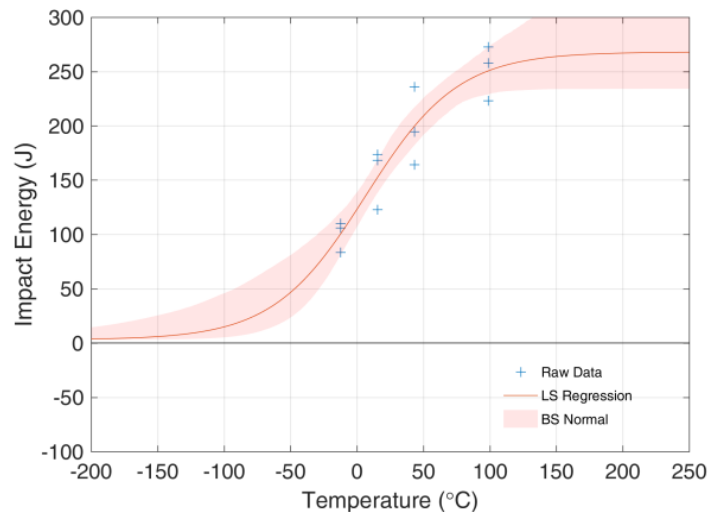
Steel  
15Kh2MFAA  
(WVER 440)



- Scatter between fracture toughness and Charpy impact shifts
  - Confirmation by IAEA-TECDOC-1435 where the scatter due to the inhomogeneous structure within the middle range of the JRQ plate 5JRQ22 plate within the  $\frac{1}{4}$ - to the  $\frac{3}{4}$ -thickness region was determined as:
    - Charpy  $T_{41}$ :  $-20^{\circ}\text{C} \pm 11.4 \text{ K}$
    - Master Curve  $T_0$ :  $-70^{\circ}\text{C} \pm 6.5 \text{ K}$
  - Both parameters  $T_{41}$  and  $T_0$  showed the same trend with strong scatter at different thickness locations, especially within the middle range.
  - It was reported in IAEA-TECDOC-1435 that the typical uncertainty in  $T_0$  (as defined in ASTM E 1921) is  $\pm 10^{\circ}\text{C}$  for the CRP data when 6 to 15 specimens have been used.



- Uncertainty assessment of  $T_{41}$  from Charpy tests by Bootstrapping is a promising tool
  - Synergies from NUGENIA+ project AGE60+
    - Charpy testing in the upper and lower shelf rather than repeat in the transition region may reduce uncertainties
    - Bootstrapping during testing may optimize the choice of test temperatures



S. Ortner et al, "Applicability of ageing related data bases and methodologies for ensuring safe operation of LWR beyond 60 years,"

[http://s538600174.onlinehome.fr/nugenia/wp-content/uploads/2016/11/22\\_AGE60+\\_V1.pdf](http://s538600174.onlinehome.fr/nugenia/wp-content/uploads/2016/11/22_AGE60+_V1.pdf)

## □ Irradiation conditions

- Neutron fluence
  - The uncertainties in determination of neutron fluence in individual irradiated specimens should have to be smaller than  $\pm 20\%$ .
  - Reliable neutron transport codes in use.
  - The effect of this uncertainty is difficult to distinguish from other effects, especially from the effect of scatter in initial condition as well as in chemical composition, and is usually covered by a margin in Embrittlement Trend Curves (ETC).

## □ Irradiation conditions

### • Neutron flux

- Neutron flux can play a non-negligible role at least for some irradiation conditions and materials.

For NiMnMo steels containing standard levels of Ni and Mn, three different scenarios are of interest as stated in the NUGENIA position paper on RPV embrittlement:

- For steels containing a low level of copper (Cu less than about 0.1%), there is no significant flux effect in a range of flux below a threshold value (about  $10^{12} \text{ n} \cdot \text{cm}^{-2} \cdot \text{s}^{-1}$ ,  $E > 1 \text{ MeV}$  at  $290 \text{ }^\circ\text{C}$ ) and irradiation temperatures between  $150$  and  $300 \text{ }^\circ\text{C}$ ;
- For steels containing a significant amount of copper and irradiated to relatively low fluence (before the saturation of copper-related hardening), three regimes are expected according to the range of flux. One can expect a flux dependence at high ( $= 7 \cdot 10^{10} \text{ n} \cdot \text{cm}^{-2} \cdot \text{s}^{-1}$ ,  $E > 1 \text{ MeV}$  at  $290 \text{ }^\circ\text{C}$ ) and low (no consensus on the threshold) flux regions, and a regime of flux independence at intermediate fluxes;
- For steels containing a significant amount of copper and irradiated to relatively high fluence (after the saturation of copper-related hardening), results support the flux independence of the copper related hardening in the saturation region. If the flux is not too high (lower than approximately  $10^{12} \text{ n} \cdot \text{cm}^{-2} \cdot \text{s}^{-1}$ ,  $E > 1 \text{ MeV}$  at  $290 \text{ }^\circ\text{C}$ ), the total hardening should be dose independent.

For steels containing high levels of Mn and Ni ( $>1.2\%$ ), results are too sparse to draw conclusions. However, it is noteworthy that results yielded by Williams and co-workers show that the embrittlement of low copper steels (Cu  $< 0.1\%$ ) with  $1.6\%$  Ni and  $1.2\text{--}1.7\%$  Mn is flux independent.

[http://s538600174.onlinehome.fr/nugenia/wp-content/uploads/2014/07/NUGENIA\\_position\\_paper\\_RPV\\_irradiation\\_embrittlement\\_May\\_2015.pdf](http://s538600174.onlinehome.fr/nugenia/wp-content/uploads/2014/07/NUGENIA_position_paper_RPV_irradiation_embrittlement_May_2015.pdf)

## □ Irradiation conditions

- Neutron flux
  - Important factor on the irradiation-induced clusters, but plays a relatively minor role (and imposes therefore less uncertainty) on the mechanical properties.
    - Increase of flux by a factor of 10 or more yields to a significant increase of the number density and a significant decrease of the size of irradiation-induced clusters.
    - The flux effect on mechanical properties is much weaker and probably insignificant, because the opposite effects of flux on cluster size and number density partly cancel out in the mechanical properties.
    - Embrittlement Trend Curves are usually based on results from testing surveillance specimens.
    - Maximum value of lead factor in RPV surveillance are given in the range between 1.5 and 5 according to the ASTM or 1.5 to 12 according to the KTA.
  - Flux decreases from the inner to the outer surface of RPV wall by a factor of the order of 5, as estimated for the NPP Greifswald Unit 4.

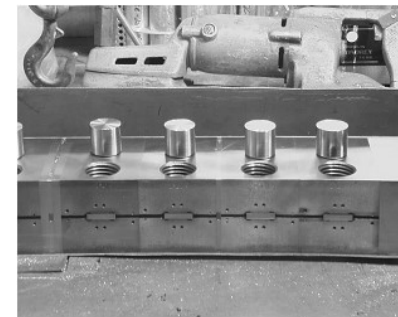
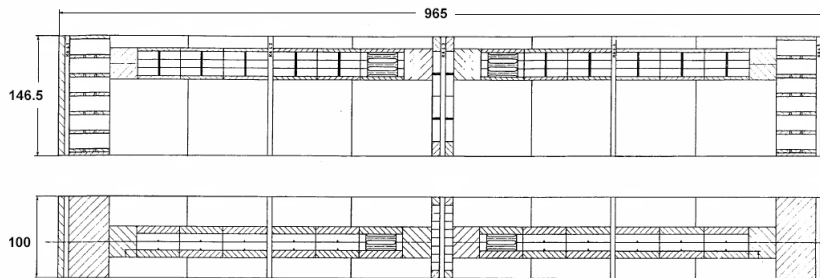


## □ Irradiation conditions

- Neutron energy spectrum
  - Effect is obvious but the experimental verification is complicated as other factors are present at the same time e.g. neutron flux.
    - IAEA CRP-1: possible effect as a result of the irradiation location since the transition temperature shifts after irradiation in out of core position (and HWR core) were generally lower than after irradiation in the core. This is in good agreement with IAEA Round-Robin Exercise (RRE) on WWER welds where the transition temperature shifts after irradiation in surveillance specimen position were smaller than after irradiation in experimental reactors.
    - In both cases irradiation in positions with a larger fluence energy ratio  $0.5\text{MeV}/1\text{MeV}$  resulted in smaller transition temperature shifts than in positions with a smaller ratio.
    - IAEA CRP-3 and KORPUS: it seems that use of fluence with  $E > 1\text{ MeV}$  is non-sensitive to the effect of neutron energy spectrum. On the contrary, fluences with  $E > 0.5\text{ MeV}$  and parameter dpa contain many neutrons with energies smaller than  $1\text{ MeV}$  that are probably much less efficient in radiation damage than neutrons with larger energies.

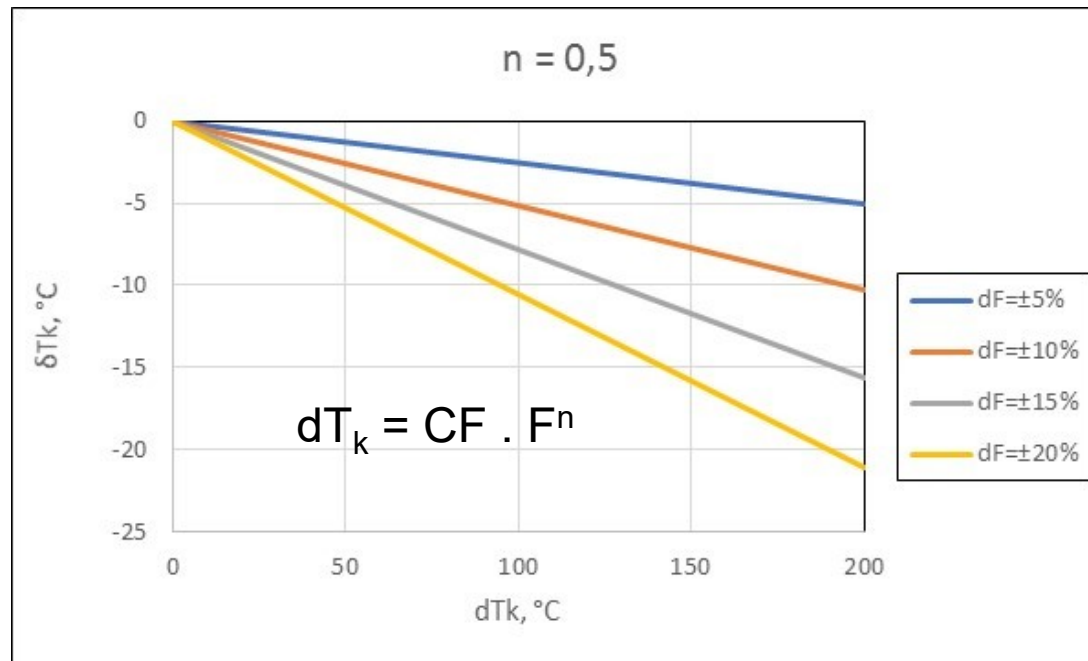
## □ Irradiation conditions

- Scatter in neutron fluence of specimens
  - The single specimens are exposed to different neutron fluences depending on the position of the specimen and the spatial neutron fluence distribution, and possible shielding effects.
  - Capsule positions of Charpy specimens of two batches of the ANP-2 and a similar material irradiated in a large VAK reactor capsule.
    - The radial shielding effect (in second specimens row) amounts to -15 % neutron fluence with deviations up to 11 % between single specimen and averaged specimen batch.
  - The impact of the axial capsule position is in general low in comparison to the radial shielding effect.



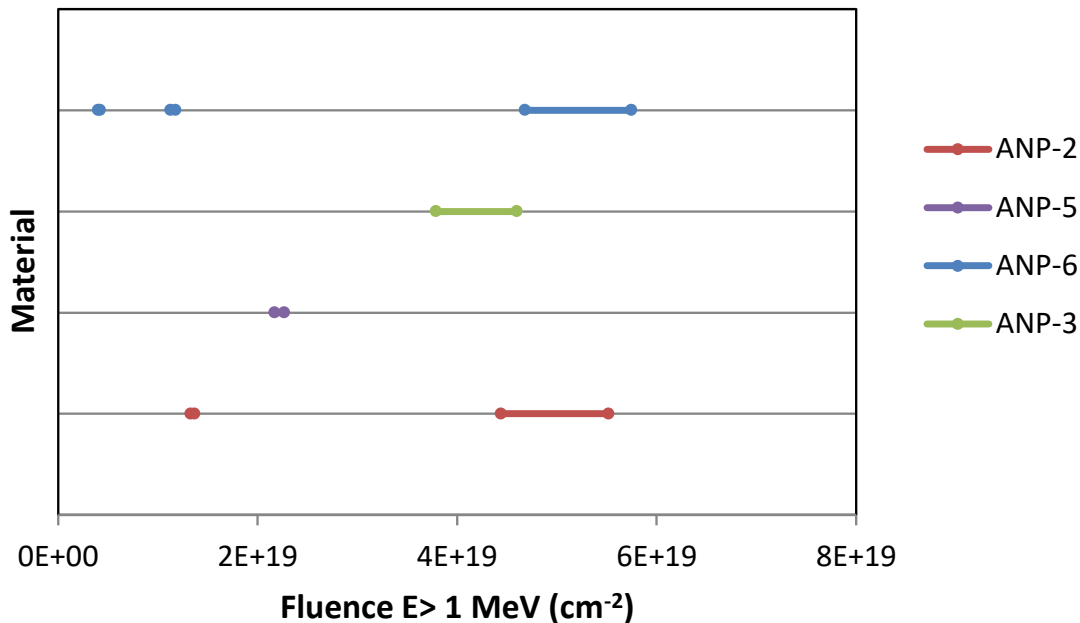
## □ Irradiation conditions

- Scatter in neutron fluence of specimens
  - Assuming  $\pm 15\%$  scatter resulting in different radiation embrittlement of individual specimens
    - Effect on the difference in transition temperature for different level of embrittlement ( $dT_k$ ) and constant slope of Embrittlement Trend Curve ( $n=0.5$ )



## □ Irradiation conditions

- Scatter in neutron fluence of specimens
  - The standard deviations of fluences ( $E > 1$  MeV) of the specimen batches from the irradiated materials ANP-2, ANP-3, ANP-5 and ANP-6 are  $\sigma < 2\%$  for four test batches, three of them are of higher scatter ( $\sigma < 9\%$ ).





## □ Irradiation temperature

- There are two sources of uncertainty related to irradiation temperature
  - Error of direct measurement (or any other way of estimation)
  - Interpretation of surveillance test results as being representative for RPV wall, operation temperature and its spatial variations
- Important to consider the effect of irradiation temperature as an uncertainty factor in surveillance testing and assessment.
  - In this context the impact of  $\gamma$ -irradiation is not significant but may cause a few K higher irradiation temperature in the surveillance specimens.

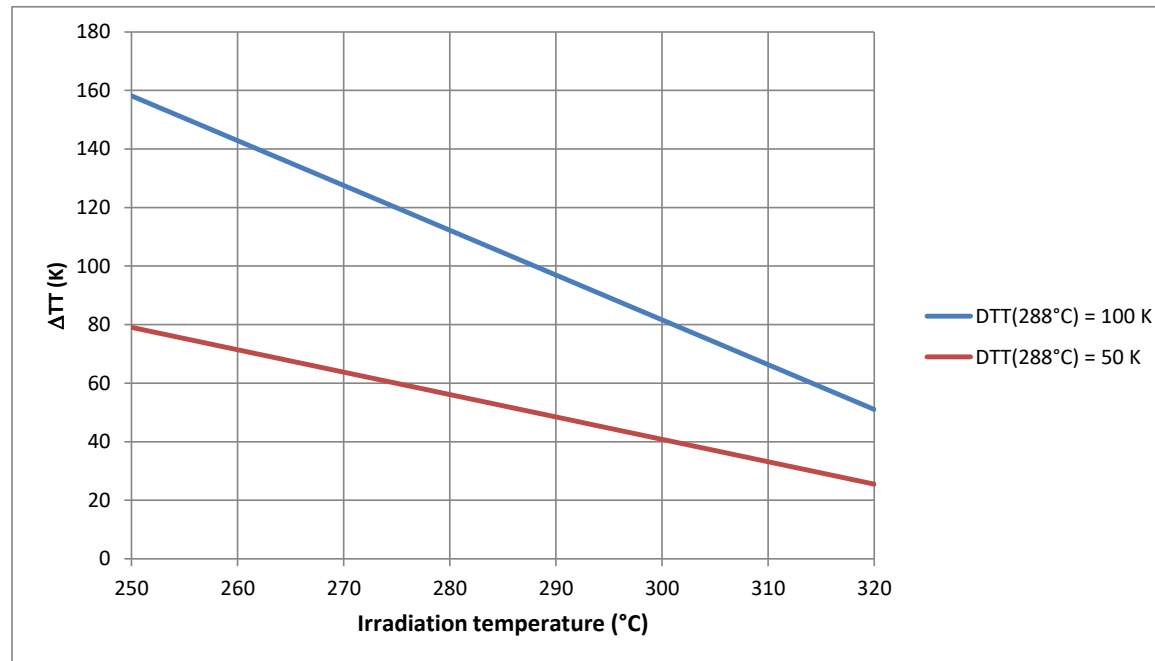
## □ Irradiation temperature

- Assuming an uncertainty of irradiation temperature of 10 K

- $\Delta T_{41} = 15$  K (if  $\Delta T_{41}$  of 100 K is assumed)
- $\Delta T_{41} = 8$  K (if  $\Delta T_{41}$  of 50 K is assumed )

$$\Delta TT = \Delta TT_{288^\circ\text{C}} (1 - 0.0153(T - 288))^*$$

- Rough approximation for well designed RPV steels under LTO
  - 1 K increase in irradiation temperature results in 1 K lower  $\Delta T_{41}$



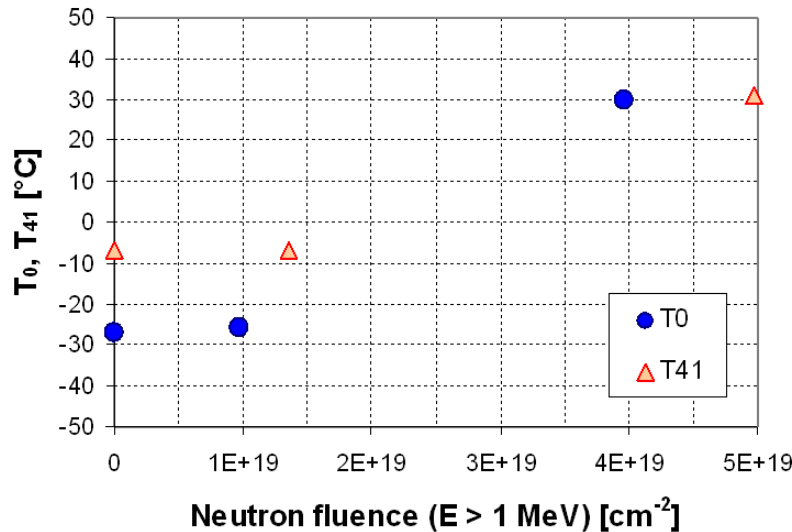
\*) Todeschini, Y. Lefebvre, H. Churier-Bossennec, N. Rupa, G. Chas, C. Benhamou, Revision of the Irradiation Embrittlement Correlation Used of the EDF RPV Fleet, Fontevraud VII, 26 – 30 September 2010, Avignon, France

## □ Removal position of specimens (I)

- ANP-2

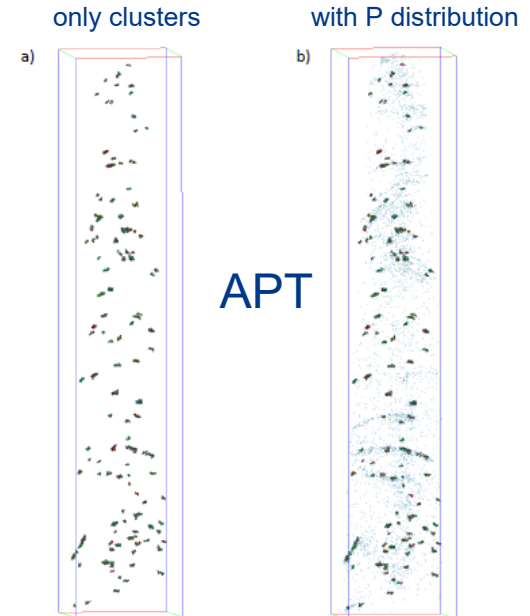
- Measured material properties confirmed by SANS and APT results
- Reason of the unexpected irradiation behaviour?

Material testing



SANS

Fluence, $\Phi$ ( $10^{19} \text{ cm}^{-2}$ ) ( $E > 1 \text{ MeV}$ )	Volume fraction, $c$ (vol%)	Number density, $N$ ( $10^{16} \text{ cm}^{-3}$ )	Radius, $R_{\text{mean}}$ (nm)	Radius, $R_{\text{peak}}$ (nm)	A-ratio
1.36	<0.005	$2 \pm 2$	-	-	$\sim 1$
4.70	$0.10 \pm 0.02$	$55 \pm 5$	0.72	0.55	$2.54 \pm 0.08$



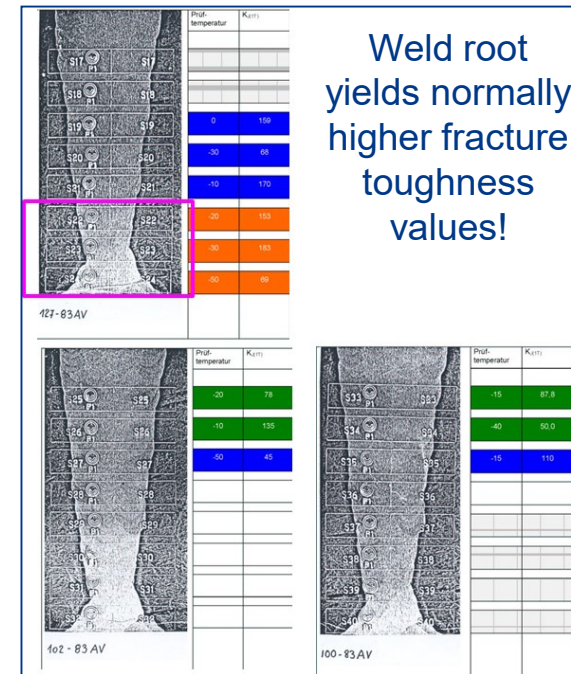
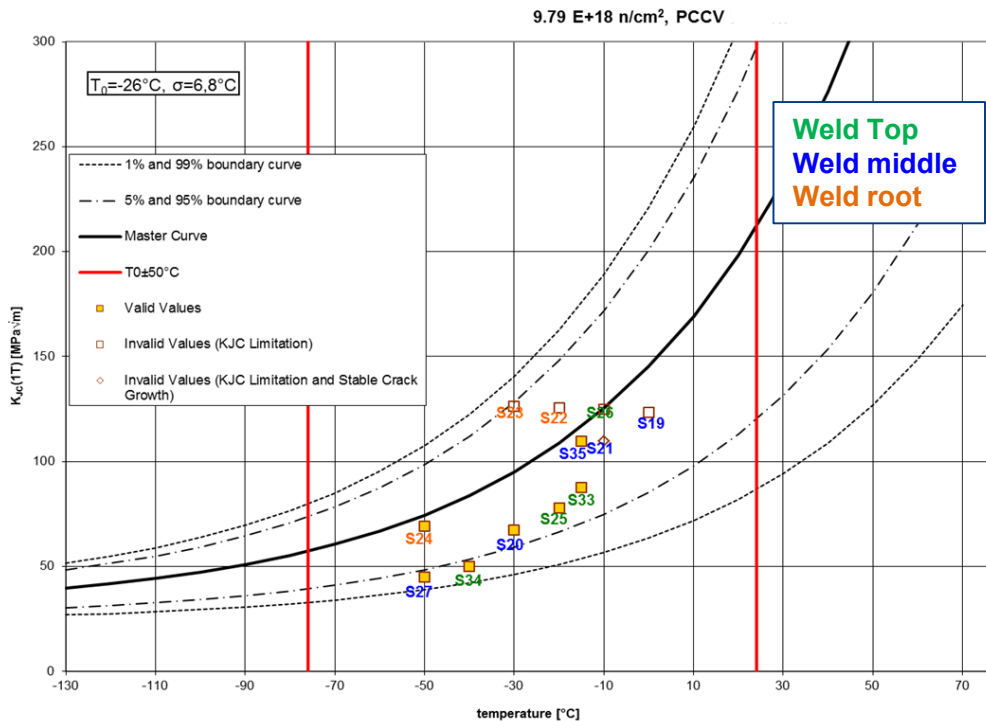
Mn/Ni/Si/Cu enriched clusters in ANP-2 irradiated to  $5 \times 10^{19} \text{ n/cm}^2$

H. Hein et al, "Some recent research results and their implications for RPV irradiation surveillance under long term operation," IAEA Technical Meeting, 5-8 November 2013, Vienna, Austria

## □ Removal position of specimens (II)

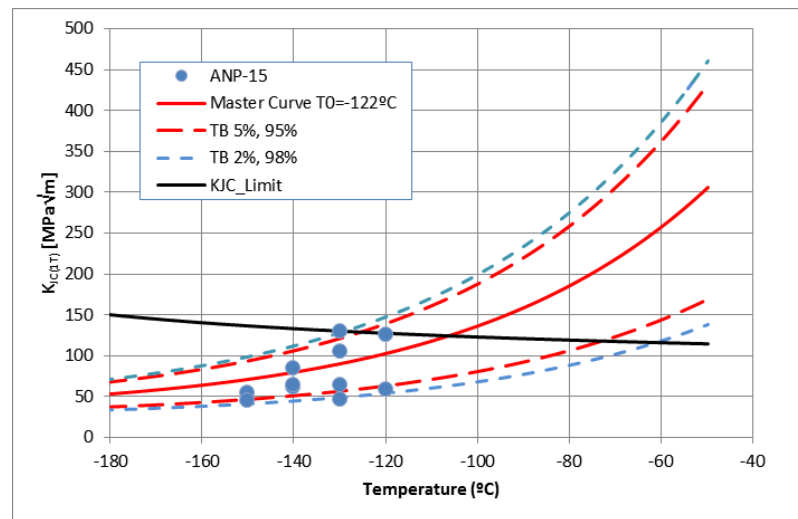
- ANP-2

- Too low  $T_0$  might be caused by use of specimens from weld root area
- $\geq 10$  K higher  $T_0$  if specimens from weld root area are omitted



## □ Thermal ageing

- May have an effect on the results of RPV irradiation surveillance programs, ANP-15 (low Cu/Ni/P forged base material) was 30 years aged at 290 °C on the cold leg of a PWR primary coolant loop
- Fracture toughness testing of ANP-15 according to ASTM E1921 results in  $T_0$  of about -120 °C confirming earlier impact test results (no thermal ageing)



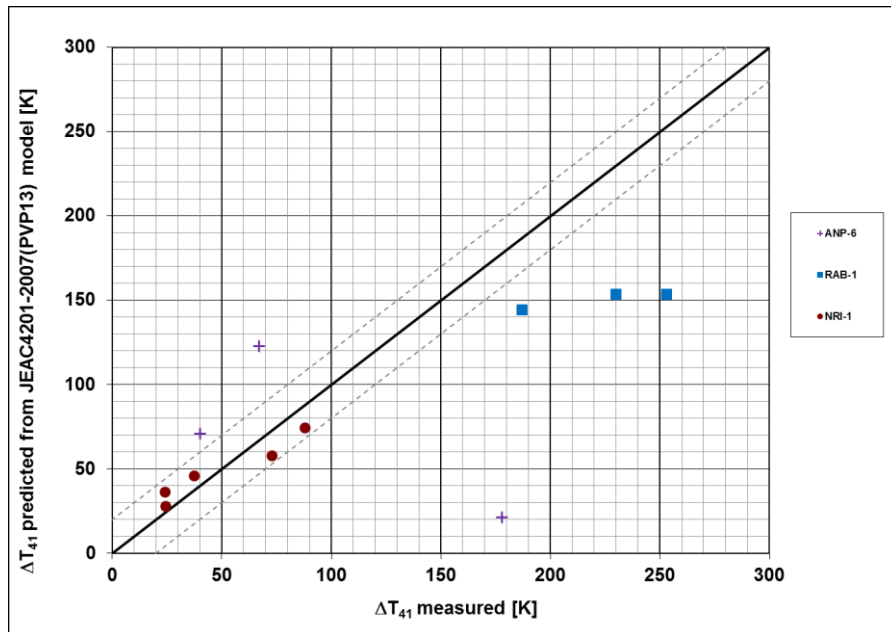
## □ Embrittlement Trend Curves

- The irradiation data (measured  $\Delta T_{41}$ ) of 14 European RPV materials was applied to 8 well-known Embrittlement Trend Curves (ETCs) with the objective to assess the appropriateness of the prediction formulas for the investigated materials.
  - ASTM E900-02, 10CFR50.61a, Wide-Range WR-C(5) Rev.1, Todeschini EDF 900 MW (FIM), Erickson Fit 6, JEAC4201-2007 (PVP13), Reg Guide 1.99 Rev. 2 and ASTM E900-15
- ETC predictions need careful application rules depending on material conditions
- The application of ETC can be connected with larger uncertainties ( $> \pm 20$  °C) in prediction of  $\Delta T_{41}$

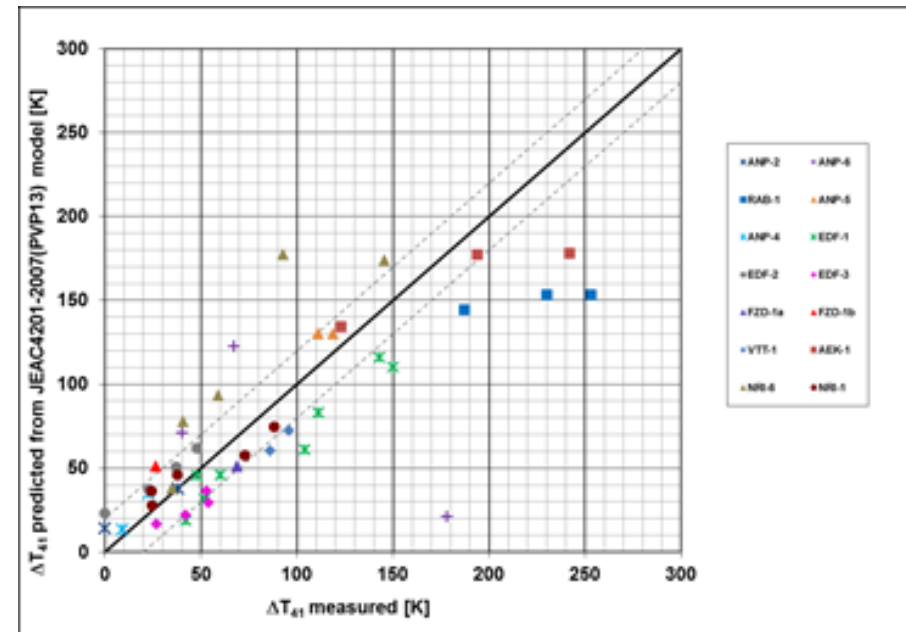
## □ Embrittlement Trend Curves

- Example: JEAC4201-2007 (PVP13)

high Ni



all materials



- ❑ An assessment of uncertainties in RPV irradiation behaviour with respect to initial microstructure, material variability and other influencing factors was performed taking into account the evaluation of results of the experimental test program and analysis of existing data done in SOTERIA WP3 with the aim to improve the reliability of RPV irradiation surveillance data.
- ❑ The main conclusions in terms of quantifiable uncertainties and scatter effects from an end user perspective are summarized as follows:

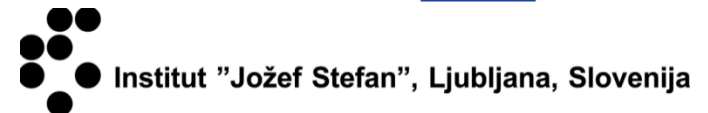
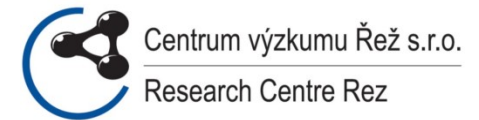


- Regarding microstructure the initial dislocation structure is heavily inhomogeneous in terms of distinct regions of low and high dislocation density, and the irradiation-induced loops tend to arrange along grain boundaries and pre-existing dislocations.
- The specimen removal position may contribute significantly to scatter in strength and toughness data.
  - For  $T_0$  an additional  $\sigma$  of about 10 °C may be expected between  $1/4$  and  $3/4$  thickness in RPV base metals.
  - Care has to be taken for specimen removal position that has to be according to the requirement of the test standards (BM shall be removed from about the quarter-thickness ( $1/4$ -T or  $3/4$ -T) locations, WM not in the root or surfaces of the welds).
- The typical uncertainty for both  $T_{41}$  and  $T_0$  is in a range of  $\pm 10$  °C.

- SINTAP and multi modal approaches are appropriate tools for inhomogeneity checks resulting in a reduced number of outliers but in an increase of  $T_0$  by using these approaches.
- Chemical analyses inhere uncertainties caused by
  - the measurement method itself, differences between heat at manufacture and surveillance material, and local inhomogeneities of the material source.
  - Significant extended relative uncertainties and significant deviations (significantly > 10 %) in content of chemical elements measured on the heat at manufacture may be expected case by case.
- Thermal aging can be excluded for low Cu/Ni/P RPV steels at operation conditions (290 °C) and is therefore no issue for the reliability of RPV irradiation surveillance programs
  - However, thermal aging may play a significant role for high Cu and high Ni RPV steels, in particular at temperature around ~320°C.

- The impact of irradiation temperature, even if well understood and having a slight effect, can be roughly estimated as 1 K higher irradiation temperature yields to 1 K lower shift in transition temperature  $\Delta T_{41}$ . The impact of  $\gamma$ -irradiation is not significant but may cause a few K higher irradiation temperature in the surveillance specimens.
- For low Cu/P/Ni base materials the primary initiation site is not characterized by a specific microstructural feature, such a precipitate or inclusion, at which brittle fracture initiated.
  - In some cases, particles were identified as fracture initiation sites, however the initiating particles are not necessarily carbides as assumed in some fracture models. In particular, some particles were shown to contain oxygen. In general, the existence of particles in initiation sited is considered as typical for weld metals.

- The application of ETC can be connected with larger uncertainties ( $> \pm 20$  °C) in prediction of  $\Delta T_{41}$ , however this uncertainty can be diminished if specific material groups (low Cu/Ni/P, high Cu, high Ni) are used. Nevertheless, the data base behind the ETC model concerned is an important factor and has to be considered for the evaluation of the results.
- From an end-user perspective it can be recommended to take into account any material inhomogeneity relating to the specimen location and the specific microstructural features if existing on the fracture surfaces for the evaluation of RPV fracture toughness results.



## **The SOTERIA Project Coordinator**

Christian ROBERTSON  
CEA  
christian.robertson@cea.fr

## **The SOTERIA Project Office**

Herman BERTRAND  
ARTIC  
bertrand@artic.eu

[www.soteria-project.eu](http://www.soteria-project.eu)

This project received funding under the Euratom  
research and training programme 2014-2018  
under grant agreement N° 661913.

